The Astrophysical Journal Letters, 884:L30 (7pp), 2019 October 20 https://doi.org/10.3847/2041-8213/ab4717

Importance of Shock Compression in Enhancing ICME's Geoeffectiveness

Mengjiao Xu[1], Chenglong Shen[1,2], Yuming Wang[1,2,3], Bingxian Luo[4,5], and Yutian Chi[1]
[1] CAS Key Laboratory of Geospace Environment, Department of Geophysics and Planetary Sciences, University of Science & Technology of China, Hefei, Anhui 230026, People's Republic of China; clshen@ustc.edu.cn
[2] CAS Center for Excellence in Comparative Planetology, University of Science and Technology of China, Hefei, People's Republic of China
[3] Mengcheng National Geophysical Observatory, School of Earth and Space Sciences, University of Science and Technology of China, Hefei, 230026, People's Republic of China
[4] National Space Science Center, Chinese Academy of Sciences, No. 1 Nanertiao Zhongguancun Haidian District, Beijing, 100190, People's Republic of China
[5] School of Astronomy and Space Science University of Chinese Academy of Sciences, Yuquan Road, Shijingshan District, Beijing, 100049, People's Republic of China
Received 2019 April 23; revised 2019 September 14; accepted 2019 September 24; published 2019 October 14

Abstract

Shock embedded interplanetary coronal mass ejections (ICMEs) are of great interest in the solar and heliosphere physics community due to their high potential to cause intense geomagnetic storms. In this work, 18 moderate to intense geomagnetic storms caused by shock-ICME complex structures are analyzed in order to show the importance of shock compression in enhancing ICMEs' geoeffectiveness. Based on the characteristics of the shocks inside ICMEs, including the shock velocity, shock normal direction, and the density compression ratio, we recover the shocked part in the ICME to the uncompressed state by using a recovery model developed by Wang et al. according to the Rankine–Hugoniot relationship. Comparing the observational data and the recovered parameters, we find that the maximum southward magnetic field in the ICME is doubled and the dawn–dusk electric field is increased 2.2 times due to the shock compression. Then, the parameters of the observed and recovered solar wind and magnetic field are, respectively, introduced into various Dst prediction models. The prediction results show that, on average, the shock compression can enhance the intensity of the geomagnetic storm by a factor of 1.4. Without shock compression, the geoeffectiveness of these ICMEs would be markedly reduced. Moreover, there is a significant correlation between the shock density compression ratio and the shock's capacity of strengthening geomagnetic storms. The larger the shock density compression ratio is, the more obvious Dst index decrease is caused.

Key words: solar–terrestrial relations – Sun: coronal mass ejections (CMEs)

1. Introduction

Due to the possible influence on the space weather effect of coronal mass ejections (CMEs), the interaction between multiple CMEs has attracted great attention in the solar physics and space weather community. One of its important influence is about the change of the CME kinematic parameters. Such kinematic variation caused by CMEs' interaction was first reported by Gopalswamy et al. (2001) based on the Large Angle and Spectrometric Coronagraph (Brueckner et al. 1995) observations from *Solar and Heliospheric Observatory* (*SOHO*; Domingo et al. 1995). They found that the propagation directions and velocities of CMEs changed significantly during the interaction process. In recent years, using the large field of view observations from *Sun Earth Connection Coronal and Heliospheric Investigation* (Howard et al. 2008) on board *Solar TErrestrial RElations Observatory* (Kaiser et al. 2008), extensive efforts further confirm the result that interaction may change the kinematic parameters of CMEs greatly (e.g., Lugaz et al. 2009, 2017; Manchester et al. 2017, and reference therein). In addition, the physics process during the interaction between CMEs has been specifically analyzed in these works. They found that the interaction process might be in-elastic, elastic or super elastic (e.g., Liu et al. 2012, 2014a; Lugaz et al. 2012; Shen et al. 2012, 2013, 2017b; Temmer et al. 2012; Mishra et al. 2015a, 2015b).

Near the Earth, the complex structures caused by the interactions between multiple CMEs are often observed. These complex structures are thought to be important sources of the geomagnetic storms, especially the intense geomagnetic storms (e.g., Wang et al. 2003b, 2005; Xue et al. 2005; Zhang et al. 2007; Lugaz et al. 2015a, 2015b; Shen et al. 2017a). One special complex structure is called a shock-interplanetary coronal mass ejection (ICME; called as S-ICME hereafter) structure, which was first reported by Ivanov (1982) and then further confirmed by Burlaga et al. (1987). In this type of complex structure, a shock driven by a following fast CME catches up and then propagates into the previous slow CME. Based on some typical events, Wang et al. (2003c) found that S-ICMEs were the main causes of some intense geomagnetic storms. Lugaz et al. (2015a) reported a case in which an extreme geomagnetic disturbance was caused by the S-ICME. Based on a statistical analysis, Lugaz et al. (2015b) confirmed the result that S-ICMEs can be an important source of intense geomagnetic storms. Based on a catalog of ICMEs and their complex structures, Shen et al. (2017a) showed that S-ICMEs can cause the geomagnetic storms, especially intense geomagnetic storms with higher possibility compared with isolated ICMEs.

But questions still remained. One major question is how much a shock can enhance the geoeffectiveness of an ICME. To answer this question, Shen et al. (2018) analyzed an intense geomagnetic storm caused by an S-ICME in 2017 September. The peak Dst index of this geomagnetic storm is −142 nT. Through recovering the shocked part of the ICME back to the uncompressed states and then substituting them into Dst prediction models, they quantitatively found that the shock compression enhanced the intensity of this geomagnetic storm by roughly a factor of two. Without shock compression, there

would be only a moderate geomagnetic storm. This study further illustrates that the S-ICME is a very important structure in solar physics study and space weather forecast.

In this work, we extend the work from Shen et al. (2018) by studying all the moderate to intense geomagnetic storms caused by S-ICMEs from 1995 to 2018. In Section 2, we will discuss a typical case in which an S-ICME caused an intense geomagnetic storm. We will also introduce the analytical methods used in this paper that were first developed in Shen2018. We will present the selection criteria for the cases that were used to make a statistical analysis in Section 3. The statistical results of these events will be shown in Section 4, including the distribution of the geomagnetic storm intensification and the relationship between the shock parameters and the geoeffectiveness enhancements. A brief discussion and conclusion are provided in the last section.

2. Method and a Typical Example

Figure 1 shows an example of the S-ICME and the associated geomagnetic disturbance: the 2012 September 30–2012 October 1 event. Liu et al. (2014b) has identified the solar and interplanetary source conditions responsible for this two-step geomagnetic storm. In their survey, two CMEs were found to interact near 1 au and formed a complex ejecta with a shock inside, which generated an intense geomagnetic storm. Furthermore, Lugaz et al. (2015a) emphasized the contribution of the shock compression to this intense two-step geomagnetic storm.

From the top to the bottom, panels in Figure 1 show the three components of the solar wind velocity, the elevation (θ) and azimuthal (ϕ) of magnetic field direction, the B_z component, the proton number density, proton β, and the Dst index adopted from the Word Data Center. Black lines in each panel represent the observational data. Seen from Figure 1, there was an ICME starting at 12:29 UT on 2012 September 30 and lasting until 09:38 UT on 2012 October 1. Shaded regions in Figure 1 show the period of this ICME. During this period, the in situ observations exhibit typical signatures of a magnetic cloud (MC) with enhanced magnetic field intensity, smooth rotated magnetic field vector, low proton density and low plasma β (e.g., Burlaga et al. 1981). According to the z component of the magnetic field, this MC is an "S-N" type MC. After the arrival of this MC, the southern component of the magnetic field B_s ($-B_z$) carried by this MC caused the first decrease of the Dst index. The Dst index reached its first peak at the time of 2012 September 30 21:00 UT with the value of −41 nT. Thereafter, a fast forward shock hit the Earth at the time of 22:18:36 UT (yellow vertical solid line). After the shock arrival, the B_s in this MC enhanced obviously from ~6 nT to ~20 nT. Seen from panel (i), the Dst index decreased quickly soon after the arrival of the shock due to the enhanced B_s. At the time of 05:00 UT on October 1, the Dst index reached its final peak with the minimum Dst value of −119 nT. Thus, this is an intense geomagnetic storm caused by the S-ICME complex structure.

To check the possible influence of the shock compression on the geomagnetic storm, we use the method developed by Shen et al. (2018). They used the model developed by Wang et al. (2018) to recover the shocked part of the ICME to the uncompressed state. The Wang et al. (2018) model relates the magnetic field, plasma velocity and density in the sheath region to the uncompressed state by applying the Rankine–Hugoniot jump conditions at the shock surface. In addition, this method assumes that the shock normal direction ($\hat{n}$), shock speed (v_s), and the shock density compression ratio (r_c) remain unchanged after entering the ICME.

Treating the shocked part of the ICME as the downstream (using subscript "2") of the shock, then the parameters in the shock upstream (using subscript "1"), that is, the restored uncompressed state, can be calculated by the following equations:

$$\rho_1 = \frac{1}{r_c}\rho_2 \tag{1}$$

$$\boldsymbol{B}_{1n} = \boldsymbol{B}_{2n} \tag{2}$$

$$\boldsymbol{B}_{1\perp} = \frac{v_{A2}^2 - u_2^2}{v_{A2}^2 - r_2 u_2^2}\boldsymbol{B}_{2\perp} \tag{3}$$

$$\boldsymbol{u}_{1n} = r_c \boldsymbol{u}_{2n} \tag{4}$$

$$\boldsymbol{u}_{1\perp} = \frac{v_{A2}^2 - u_2^2}{v_{A2}^2 - r_2 u_2^2} r_c \boldsymbol{u}_{2\perp}. \tag{5}$$

Here, ρ is the density, v_A is the Alfvén speed, $\boldsymbol{B}$ represents the magnetic field, and $\boldsymbol{u}$ is the solar wind speed in the deHoffman-Teller (HT) frame. The HT frame varies as the shock propagates in the ICME. It is determined by the magnetic field and velocity field data at different times. The subscripts "n" and "$\perp$" mean the component parallel and perpendicular to the shock normal. The recovered interval is longer than the observed shocked interval, and its duration is calculated based on the mass conservation with the formula of $dt_1 = \frac{u_{2n}+v_s}{u_{1n}+v_s} r_c dt_2$.

Supposing that the shock parameters ($\hat{n}$, v_s, r_c) remain constant after entering the ICME, the uncompressed state of the ICME can be calculated through substituting the shock parameters fitted at the observed shock surface into the above functions. After getting the uncompressed state of the ICME, we can then substitute it together with the observed compressed ICME into various Dst index prediction models, as illustrated in Shen et al. (2018), to quantitatively estimate the enhancement of a geomagnetic storm caused by shock compression.

To obtain the shock parameters, we adopt nonlinear least-squares fitting of the incomplete Rankine–Hugoniot (R–H) relations (temperature information is not used) written in shock frame. This shock fitting method was originally developed by Vinas & Scudder (1985) and further enhanced by Szabo (1994). Based on this method, we can get the normal direction, the shock speed, and the compression ratio of the shock. Applying this method to the shock recorded by Wind at 22:18:36 UT on 2012 September 30, we get that the shock normal direction ($\hat{n}$) in Geocentric Solar Magnetospheric coordinate is [−0.91, 0.42, −0.07], shock speed (v_s) is 446 km s^{-1} and density compression ratio (r_c) is 2.11.

In Figure 1, the red curves in panels (a) to (g) between the yellow solid line and the yellow dashed line show the recovered parameters. The yellow dashed vertical line represents the recovered ICME trailing edge. According to the in situ observations, the peak values of B_s and E_y in this ICME are 20.5 nT and −8.1 mv m^{-1} respectively. But, in the recovered results, the peak values of B_s and E_y decreased to 9.6 nT and −3.4 mv m^{-1}. Since B_s and E_y are main factors in determining the intensity of a geomagnetic storm (e.g., Gonzalez et al. 1994; Wang et al. 2003a; Shen et al. 2017a), we can expect that the entrance of the shock significantly enhances the intensity of this geomagnetic storm.

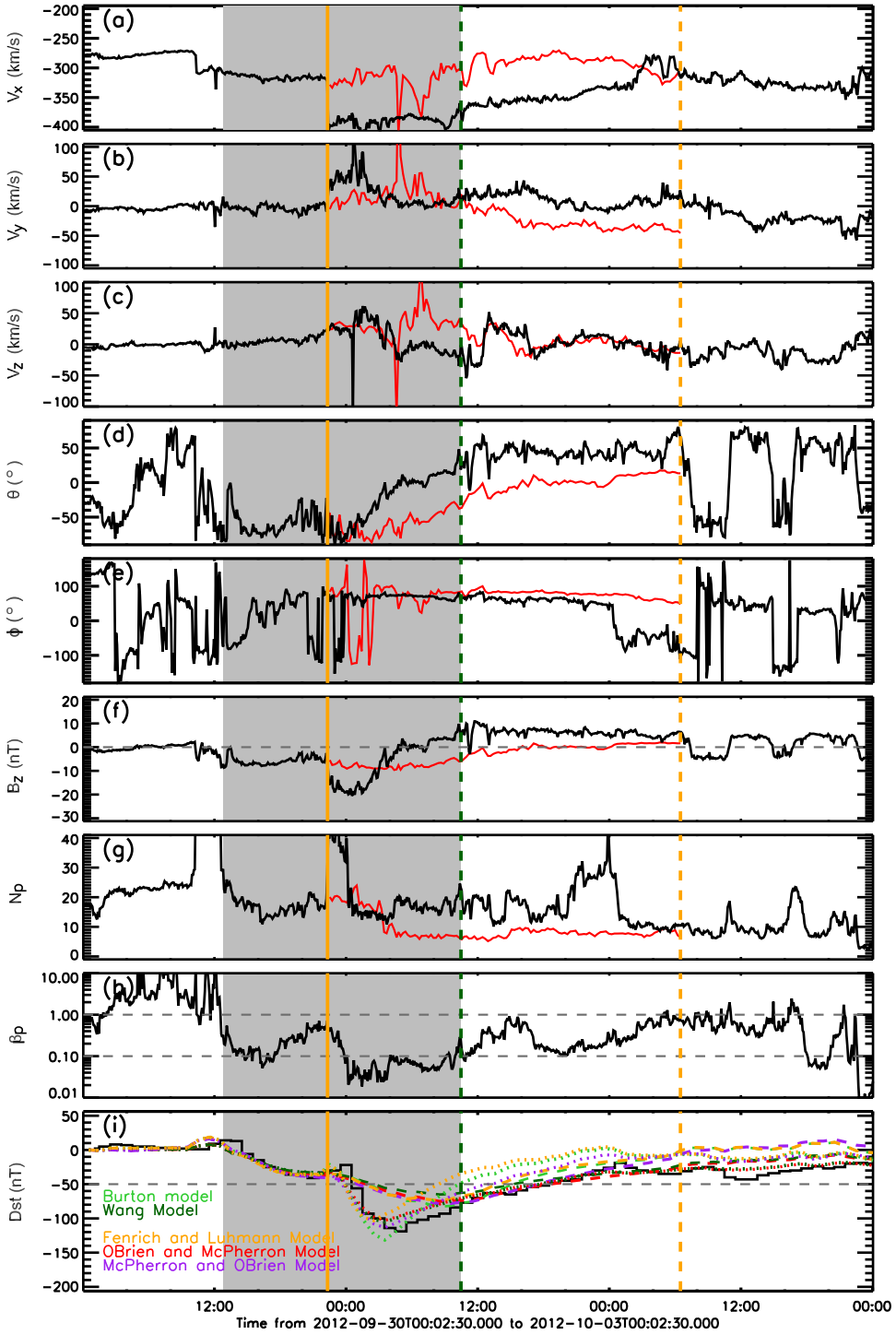

Figure 1. Observational data and recovered uncompressed state of magnetic field, solar wind speed, total plasma density, and Dst index from 2012 September 30 to 2012 October 2. The shaded region shows the period of the ICME. The black lines in panels (a) through (h) show the original observations, and the red lines between the yellow solid and yellow dashed vertical lines represent the recovered parameters. The green and yellow dashed vertical lines mark the ICME end time based on observational and reconstructed data. Panel (i) shows the real data (black line) and the prediction results based on the observed (dotted lines) and recovered (dashed lines) parameters of the Dst index. Different colors represent different prediction methods.

Panel (i) in Figure 1 shows the predicted Dst indices based on the observed solar wind and magnetic field data (colored dotted curves) and restored parameters (colored dashed curves). Different colors represent different Dst prediction models, which are the Burton model (Burton et al. 1975), the Fenrich and Luhmann (FL) model (Fenrich & Luhmann 1998), the O'Brien and McPherron (OBM) model (O'Brien & McPherron 2000), the McPherron and O'Brien (MOB) model (McPherron & O'Brien 2001), and the Wang model (Wang et al. 2002).

As seen from the dotted lines in Figure 1(i), all these models can well predict the variation of the Dst index based on the observations of the interplanetary parameters. The peak values of the predicted Dst index based on observations are also

similar with the observed Dst index. They are −131 nT, −103 nT, −103nT, −113 nT, and −105 nT for Burton model, FL model, OBM model, MOB model, and Wang model respectively. But, compared to the prediction results based on the solar wind observations, the predicted Dst indices based on the recovered parameters decrease much slower. The peak values of the Dst index are −83 nT, −74 nT, −75 nT, −79 nT, and −65 nT, respectively. This means that the peak values of the Dst indices decrease by factors of 1.6, 1.4, 1.4, 1.4, and 1.6 in different models. On average, the shock compression enhances the intensity of the geomagnetic storm by a factor of 1.5. Without shock compression, there would be only a moderate geomagnetic storm with a peak Dst value of about −76 nT.

3. Events Selection

To make a statistical analysis, we first select all S-ICMEs from 1995 to 2018 based on the Wind Observations. The S-ICMEs are adopted from the ICMEs catalog generated and maintained at the University of Science and Technology of China (USTC). This catalog was first published by Chi et al. (2016) and then extended to the end of 2018 by Xu et al. (2019). The online catalog can be found at http://space.ustc.edu.cn/dreams/wind_icmes/. In this catalog, all ICMEs are divided in to three types: (i) isolated ICMEs (I-ICMEs); (ii) multiple ICMEs (M-ICMEs), and (iii) shock-ICMEs (S-ICMEs) (Shen et al. 2017a). During the period from 1995 to 2018, there are a total of 58 S-ICMEs in USTC's ICME catalog.

In order to find the importance of the shock compression in enhancing the geoeffectiveness of ICMEs, the S-ICMEs used in further analysis should satisfy the following criteria. (i) The S-ICMEs should cause moderate to intense geomagnetic storms with the peak Dst values less than −50 nT. By this criterion, we excluded 22 events. In those events, ICMEs do not carry, or carry very weak, southward magnetic field; therefore, no moderate to intense geomagnetic storms are caused. (ii) The main phases of the geomagnetic storms should be primarily caused by the shock compressed part of the ICMEs instead of the uncompressed parts or the regions after the ICME. In these cases, we can say for sure that shocks play important roles in enhancing the ICMEs' geoeffectiveness. According to this criterion, another 18 events are eliminated. Such a screening method allows us to eventually find 18 moderate to intense geomagnetic storms triggered by S-ICMEs. These 18 S-ICMEs are then studied with the methods described in Section 2, including fitting shock parameters, recovering the shocked part of the ICME and predicting Dst indices.

4. Statistical Results

The information of these 18 events are listed in Table 1, including the ICME and shock parameters of these 18 events, the enhancements of the maximum and mean southward magnetic field and dawn–dusk electric field due to the shock compression as well as the predicted peak Dst indices. Columns in Table 1 show from left to right, the start and end times of the ICME (ICME_beg, ICME_end), the shock arrival time, the shock speed (v_s), the density compression ratio (r_c), the angle between the shock normal and the upstream magnetic field direction (θ_{Bn}), the ratio between the observed and recovered maximum and mean southward magnetic field (B_s) and dawn–dusk electric field (E_y), and the predicted peak Dst indices based on the observational and recovered conditions with the five Dst prediction models. The last column shows the time interval between predicted Dst peak time using the recovered parameters and the observational data (Δt). Here, positive Δt means that the predicted Dst peak time using the recovered state is later than the predicted Dst peak time using the observational data. Besides, there are three cases in which the Dst index will not peak without shock compression. In these three cases, the predicted Dst indices based on the recovered data are shown to be the recovery phase of geomagnetic storms. In the other 15 events, Δt are positive, indicating that shock compression makes the geomagnetic storms peak earlier.

Figure 2 indicates the contributions of the shocks to enhancing ICME's geoeffectiveness in these 18 events.

The red profiles in panels (a)–(d) show the distributions of the mean values of deviations and ratios between the measured and recovered B_s and E_y, while the black profiles indicate the distributions of the deviations and ratios between the measured and recovered peak values of B_s and E_y. On average, the maximum values of B_s are enhanced by a factor of 2.0 due to the shock compression.

Panels (e) and (f) exhibit the deviations and ratios between the peak values of the predicted Dst indices based on observations and recovered states. It includes all the prediction results from the five different Dst prediction models. The peak Dst indices of these geomagnetic storms are enhanced about 1.4 times due to the shock compression. The largest value of $r_{\rm Dst}$ is 3.04. It is also worth noting that based on the observation, 11 of the 18 events are intense geomagnetic storms ($\rm Dst_{min} \leqslant -100$ nT) and 7 are moderate geomagnetic storms ($-100\,{\rm nT} < \rm Dst_{min} \leqslant -50$ nT). However, based on the predicted Dst indices using recovered interplanetary parameters, we find that in the absence of shock compression, 5 (45%) intense geomagnetic storms will degenerate into moderate geomagnetic storms and 3 (43%) moderate geomagnetic storms will degenerate into weak geomagnetic storms. These statistical results fully demonstrate that shock-ICME interaction can effectively enhance the intensity of magnetic storms.

The scatter plots in Figure 3 show the correlations between r_c and the enhancements of the maximum (black diamonds) and mean (red triangles) values of B_s (r_{B_s}), the enhancements of the maximum (black diamonds) and mean (red triangles) values of E_y (r_{E_y}), and the enhancements of the peak Dst indices ($r_{\rm Dst}$). The correlation coefficients are shown in the lower right corner of each panel. These parameters are all highly correlated, representing that the higher the density compression ratio of the shock, the stronger its capability to strengthen geomagnetic storms. In addition, we also perform the linear fitting for each set of parameters. The results are all of high quality. The plus in each panel represents the point of (1, 1). In theory, the linear fitting result should pass through this point because a density compression ratio of one represents no compression. Seen from the figure, our fitting results agree well with this; therefore, we believe that we can roughly estimate the intensification of geomagnetic storms just by the shock density compression ratios.

Table 1
Parameters of 18 Shock-ICME Structures Associated with Moderate to Intense Geomagnetic Storms

ICME Information		Shock Parameter				B_s Increase		E_y Increase		Predicted Dst Peak using Observation/Recovered Data					Δt
ICME_beg	ICME_end	Time	V_s	r_c	θ_{Bn}	Mean	Max	Mean	Max	Burton	FL	OBM	MOB	Wang	
1995-03-04T11:42	03-05T00:08	03-04T19:59	461	1.4	78	1.4	1.4	1.5	1.5	−82/−74	−92/−89	−76/−71	−83/−75	−80/−72	1
1998-05-02T11:48	05-04T05:01	05-03T17:02	470	3.7	52	3.8	3.4	4.4	1.8	−248/−156	−307/−184	−180/−122	−230/−156	−233/−158	38
1998-11-07T22:21	11-08T11:24	11-08T04:41	694	1.5	58	1.4	1.5	1.6	1.8	−179/−165	−140/−96	−136/−125	−154/−137	−140/−120	1
1999-02-17T12:22	02-18T10:30	02-18T02:48	699	3.2	43	3.2	3.5	5.5	4.7	−184/−61	−164/−68	−140/−67	−164/−68	−149/−71	28
1999-08-21T15:18	08-23T14:06	08-22T23:27	345	1.3	84	1.3	1.3	1.3	1.3	−102/−90	−83/−72	−88/−81	−93/−85	−72/−65	1
1999-11-12T19:00	11-13T20:26	11-13T12:48	470	1.9	70	1.9	2.1	2.1	2.3	−123/−68	−65/−55	−103/−69	−112/−71	−88/−57	…
2000-04-24T04:25	04-24T13:39	04-24T09:13	562	1.6	75	2.0	1.8	2.1	2.0	−73/−50	−69/−50	−65/−50	−67/−53	−66/−46	3
2000-10-03T12:09	10-05T06:27	10-04T14:22	473	1.4	82	1.4	1.4	1.5	1.5	−140/−113	−99/−110	−112/−99	−120/−101	−114/−98	…
2000-10-03T12:09	10-05T06:27	10-05T03:28	560	2.2	81	2.2	2.3	3.0	2.9	−167/−116	−153/−91	−129/−102	−153/−105	−149/−99	…
2002-08-01T11:33	08-02T03:43	08-01T23:09	497	2.0	70	2.0	2.0	2.1	2.1	−61/−52	−52/−46	−65/−57	−60/−55	−60/−49	4
2002-08-19T18:53	08-21T21:45	08-20T13:50	495	1.2	45	1.2	1.2	1.3	1.2	−115/−97	−100/−79	−99/−89	−102/−90	−84/−72	5
2003-05-29T13:00	05-30T00:04	05-29T18:31	824	1.9	76	1.9	1.9	2.2	2.2	−161/−121	−304/−129	−128/−107	−169/−133	−214/−148	3
2003-06-17T19:03	06-18T09:04	06-18T04:42	496	1.4	60	1.5	1.5	1.6	1.6	−132/−112	−113/−69	−110/−97	−125/−106	−113/−93	2
2010-02-15T11:53	02-15T22:28	02-15T17:39	389	1.6	67	1.6	1.7	1.9	1.9	−66/−52	−64/−44	−59/−48	−67/−54	−53/−40	2
2012-09-30T12:29	10-01T09:38	09-30T22:18	446	2.1	70	2.1	2.1	2.6	2.4	−131/−83	−103/−74	−103/−75	−113/−79	−105/−65	5
2014-02-18T14:43	02-19T09:45	02-19T03:09	603	1.7	86	1.7	1.7	2.1	2.1	−122/−91	−78/−73	−99/−82	−112/−85	−93/−67	3
2014-02-19T11:43	02-20T05:51	02-20T02:42	760	2.2	83	2.2	1.9	2.5	2.9	−55/−39	−58/−34	−68/−52	−64/−49	−68/−49	3
2017-09-07T19:44	09-08T01:00	09-07T22:28	744	2.0	54	2.0	2.3	2.5	3.0	−218/−142	−193/−76	−156/−108	−177/−119	−156/−91	3

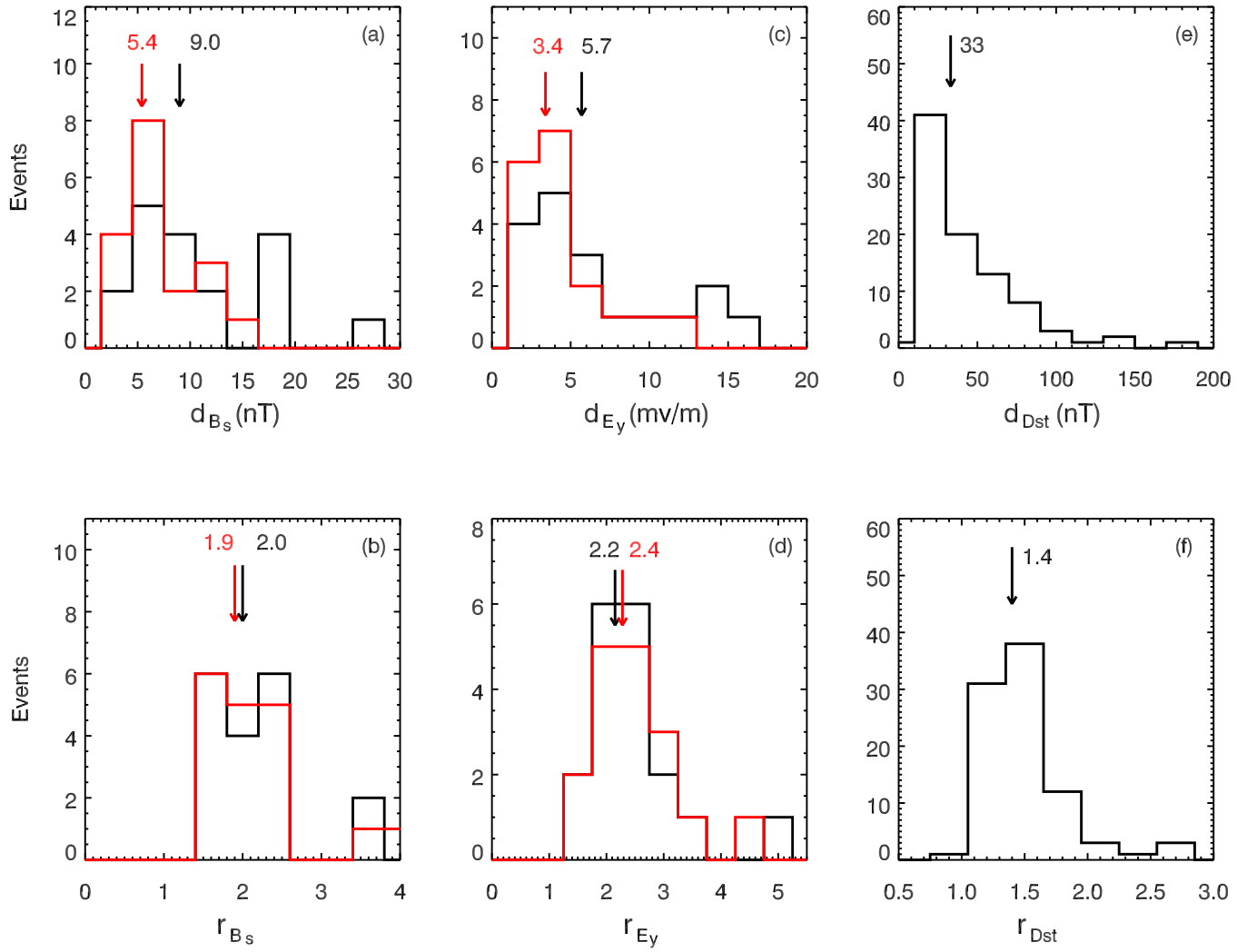

Figure 2. Distribution of the deviation (a) and ratio (b) between the measured and recovered maximum (black) and mean (red) southward magnetic field strength B_z, the deviation (c) and ratio (d) between the measured and recovered maximum (black) and mean (red) dawn–dusk electric field (E_y), and the deviation (e) and ratio (f) between the peak Dst value. The mean values are indicated by the black and red arrows in each panel.

5. Discussion and Conclusion

In this work, we analyze 18 events of moderate to intense geomagnetic storms caused by the interactions between shocks and ICMEs observed by *WIND* satellites since 1995. The main results are:

1. Based on the method put forward by Wang et al. (2018) and Shen et al. (2018), we recover the parameters of solar wind and magnetic field in the ICME intervals to their uncompressed state based on the parameters of shocks inside ICMEs. Our statistical results show that due to the compression of the shock, the maximum values of southward magnetic field in ICMEs are increased about 2 times, and those of the dawn–dusk electric field electric field increase about 2.2 times.
2. The parameters of observed solar wind and magnetic field, as well as the recovered solar wind and magnetic field parameters, are respectively introduced into various Dst prediction models. The simulated results of these models show that the shock compressions enhanced the intensities of these geomagnetic storms by a factor of 1.4 from statistical view. Without shock compression, the geomagnetic effects of these ICMEs would be significantly reduced. This confirms the results that the shock compression would significantly enhance the geoeffectiveness of ICMEs. Furthermore, in all events, shock compression makes the Dst indices peak in advance.
3. There is a significant correlation between shock density compression ratio and the shock's ability to strengthen geomagnetic storms. The higher the density compression ratio of shock, the more obvious the enhancement of the geomagnetic storm.

It should be noted that, in this work, we consider the shock compression to be a vital factor to enhance a geomagnetic storm. However, as Wang et al. (2018) mentioned, the method of recovering the shocked structure is highly ideal. On one hand, this model assumes that the shock properties in the region between the shock and ICME trailing edge are the same as those at the observed shock surface. However, due to the relatively large Alfvén speed in ICMEs, shocks will be weakened during the propagation inside (Lugaz et al. 2015b). So the shocks should be stronger at the earlier time when it just propagated into the ICME. Since there is a significant correlation between shock density compression ratio and the

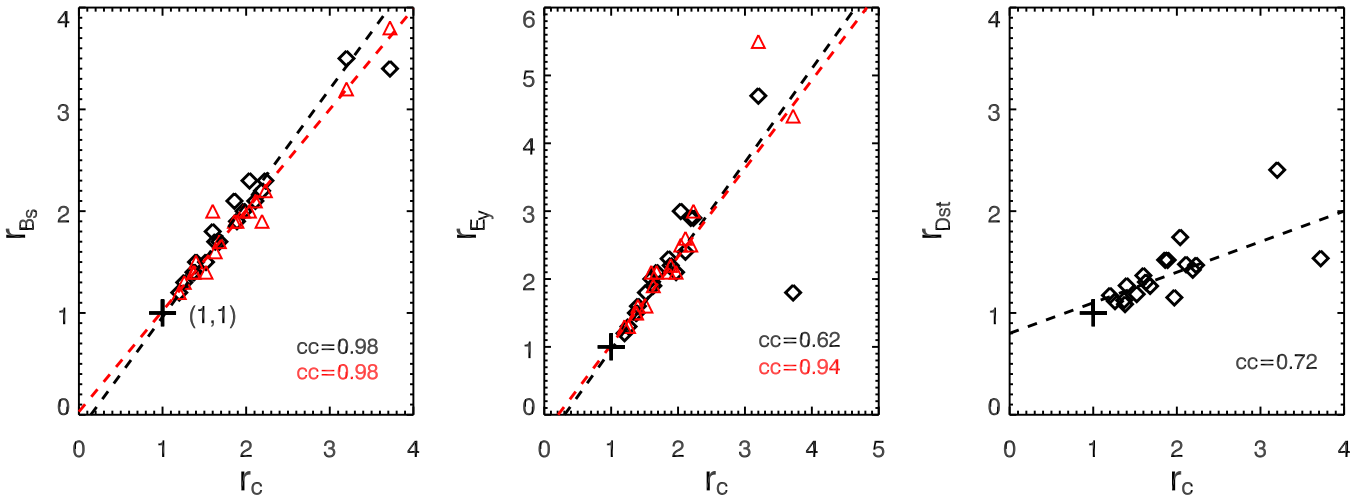

Figure 3. Correlations between r_c and the the enhancements of the maximum (black diamonds) and mean (red triangles) values of B_s (left), the enhancements of the maximum (black diamonds) and mean (red triangles) values of E_y (middle), and the enhancements of peak Dst indices (right). The correlation coefficients are shown in the lower right corner of each panel. The pluses represent the points of (1, 1).

shock's capacity to enhance geomagnetic storms, the assumption of constant shock parameters in the whole period after the shock might lead to an underestimation of shocks' contributions to the geomagnetic storms. On the other hand, the shocked part of the ICME will be restored when the shock passes away. Thus, the recovered B_z and E_y may be smaller than in a real uncompressed situation if we use the observations as the shocked parameters. In this case, we may sometimes overestimate the role of the shock in enhancing geomagnetic storms.

In addition, we find that the shock compression makes the peak time of the geomagnetic storms arrive earlier. In particular, in the S-ICME that began on 1998 May 2 (second event in Table 1), the peak time of the Dst index occurred 38 hr earlier due to the shock compression. This further suggests that shock compression is an important factor in forecasting geomagnetic storms caused by ICMEs.

The authors thank the referee for the comments that helped to improve this paper. This work is supported by grants from CAS (Key Research Program of Frontier Sciences QYZDB-SSW-DQC015), NSFC (41822405, 41774181, 41774178, 41574165, 41761134088), the Fundamental Research Funds for the Central Universities (WK2080000077), the Specialized Research Fund for State Key Laboratories and the key research program of the CAS (XDPB11), and the Specialized Research Fund for Beijing Municipal Science and Technology Project (Z181100002918004).

References

Brueckner, G. E., Howard, R. A., Koomen, M. J., et al. 1995, SoPh, 162, 357
Burlaga, L., Behannon, K., & Klein, L. 1987, JGRA, 92, 5725
Burlaga, L., Sittler, E., Mariani, F., & Schwenn, R. 1981, JGRA, 86, 6673
Burton, R. K., Mcpherron, R. L., & Russell, C. T. 1975, JGR, 80, 4204
Chi, Y., Shen, C., Wang, Y., & Ye, P. 2016, SoPh, 291, 2419
Domingo, V., Fleck, B., & Poland, A. I. 1995, SoPh, 162, 1
Fenrich, F., & Luhmann, J. 1998, GeoRL, 25, 2999
Gonzalez, W. D., Joselyn, J. A., Kamide, Y., et al. 1994, JGR, 99, 5771
Gopalswamy, N., Yashiro, S., Kaiser, M. L., Howard, R. A., & Bougeret, J. L. 2001, ApJL, 548, L91
Howard, R. A., Moses, J. D., Vourlidas, A., et al. 2008, SSRv, 136, 67
Ivanov, K. G. 1982, SSRv, 32, 49
Kaiser, M. L., Kucera, T. A., Davila, J. M., et al. 2008, SSRv, 136, 5
Liu, Y. D., Luhmann, J. G., Kajdič, P., et al. 2014a, NatCo, 5, 3481
Liu, Y. D., Luhmann, J. G., Moestl, C., et al. 2012, ApJL, 746, L15
Liu, Y. D., Yang, Z., Wang, R., et al. 2014b, ApJL, 793, L41
Lugaz, N., Farrugia, C. J., Davies, J. A., et al. 2012, ApJ, 759, 68
Lugaz, N., Farrugia, C. J., Huang, C., & Spence, H. E. 2015a, GeoRL, 42, 4694
Lugaz, N., Farrugia, C. J., Smith, C. W., & Paulson, K. 2015b, JGRA, 120, 2409
Lugaz, N., Temmer, M., Wang, Y., & Farrugia, C. J. 2017, SoPh, 292, 64
Lugaz, N., Vourlidas, A., & Roussev, I. I. 2009, AnGeo, 27, 3479
Manchester, W., Kilpua, E. K., Liu, Y. D., et al. 2017, SSRv, 212, 1159
McPherron, R. L., & O'Brien, P. 2001, GMS, 125, 339
Mishra, W., Srivastava, N., & Chakrabarty, D. 2015a, SoPh, 290, 527
Mishra, W., Srivastava, N., & Singh, T. 2015b, JGRA, 120, 10221
O'Brien, T. P., & McPherron, R. L. 2000, JASTP, 62, 1295
Shen, C., Chi, Y., Wang, Y., Xu, M., & Wang, S. 2017a, JGR, 122, 5931
Shen, C., Wang, Y., Wang, S., et al. 2012, NatPh, 8, 923
Shen, C., Xu, M., Wang, Y., Chi, Y., & Luo, B. 2018, ApJ, 861, 28
Shen, F., Shen, C., Wang, Y., Feng, X., & Xiang, C. 2013, GeoRL, 40, 1457
Shen, F., Wang, Y., Shen, C., & Feng, X. 2017b, SoPh, 292, 104
Szabo, A. 1994, JGRA, 99, 14737
Temmer, M., Vršnak, B., Rollett, T., et al. 2012, ApJ, 749, 57
Vinas, A. F., & Scudder, J. D. 1985, JGRA, 91, 39
Wang, C., Chao, J., Chen, H., et al. 2002, ChJG, 45, 793
Wang, Y., Shen, C., Liu, R., et al. 2018, JGRA, 123, 3238
Wang, Y., Shen, C. L., Wang, S., & Ye, P. Z. 2003a, GeoRL, 30, 2039
Wang, Y., Ye, P., Zhou, G., et al. 2005, SoPh, 226, 337
Wang, Y. M., Ye, P. Z., & Wang, S. 2003b, JGRA, 108, 1370
Wang, Y. M., Ye, P. Z., Wang, S., & Xue, X. H. 2003c, GeoRL, 30, 2039
Xu, M., Shen, C., Chi, Y., et al. 2019, ApJ, in press
Xue, X. H., Wang, Y., Ye, P. Z., Wang, S., & Xiong, M. 2005, P&SS, 53, 443
Zhang, J., Richardson, I., Webb, D., et al. 2007, JGRA, 112, A10102